





## Article

# Combined Electro-Fenton and Anodic Oxidation Processes at a Sub-Stoichiometric Titanium Oxide (Ti<sub>4</sub>O<sub>7</sub>) Ceramic Electrode for the Degradation of Tetracycline in Water

Busisiwe N. Zwane <sup>1,2,3</sup>, Benjamin O. Orimolade <sup>1</sup>, Babatunde A. Koiki <sup>1</sup>, Nonhlangabezo Mabuba <sup>1,3</sup>, Chaimaa Gomri <sup>4</sup>, Eddy Petit <sup>4</sup>, Valérie Bonniol <sup>4</sup> , Geoffroy Lesage <sup>4</sup> , Matthieu Rivallin <sup>4</sup>, Marc Cretin <sup>4,\*</sup>  and Omotayo A. Arotiba <sup>1,3,\*</sup> 

<sup>1</sup> Department of Chemical Sciences, University of Johannesburg, Doornfontein, Johannesburg 2028, South Africa; nokalika.zwane@gmail.com (B.N.Z.); orimoladeben@yahoo.com (B.O.O.); bakoiki@gmail.com (B.A.K.); nmabuba@uj.ac.za (N.M.)

<sup>2</sup> DST/Mintek Nanotechnology Innovation Centre, University of Johannesburg, Johannesburg 2028, South Africa

<sup>3</sup> Centre for Nanomaterials Science Research, University of Johannesburg, Johannesburg 2028, South Africa

<sup>4</sup> Institut Européen des Membranes, IEM, Univ Montpellier, CNRS, ENSCM, 34095 Montpellier, France; chaimaa.gomri@umontpellier.fr (C.G.); eddy.petit@umontpellier.fr (E.P.); valerie.bonniol@umontpellier.fr (V.B.); geoffroy.lesage@umontpellier.fr (G.L.); matthieu.rivallin@umontpellier.fr (M.R.)

\* Correspondence: marc.cretin@umontpellier.fr (M.C.); oarotiba@uj.ac.za (O.A.A.); Tel.: +27-11-559-6200 (O.A.A.)



**Citation:** Zwane, B.N.; Orimolade, B.O.; Koiki, B.A.; Mabuba, N.; Gomri, C.; Petit, E.; Bonniol, V.; Lesage, G.; Rivallin, M.; Cretin, M.; et al. Combined Electro-Fenton and Anodic Oxidation Processes at a Sub-Stoichiometric Titanium Oxide (Ti<sub>4</sub>O<sub>7</sub>) Ceramic Electrode for the Degradation of Tetracycline in Water. *Water* **2021**, *13*, 2772. <https://doi.org/10.3390/w13192772>

Academic Editor: Zacharias Frontistis

Received: 24 August 2021

Accepted: 23 September 2021

Published: 6 October 2021

**Publisher's Note:** MDPI stays neutral with regard to jurisdictional claims in published maps and institutional affiliations.



**Copyright:** © 2021 by the authors. Licensee MDPI, Basel, Switzerland. This article is an open access article distributed under the terms and conditions of the Creative Commons Attribution (CC BY) license (<https://creativecommons.org/licenses/by/4.0/>).

**Abstract:** The mineralization of tetracycline by electrochemical advanced oxidation processes (EAOPs) as well as the study of the toxicity of its intermediates and degradation products are presented. Electro-Fenton (EF), anodic oxidation (AO), and electro-Fenton coupled with anodic oxidation (EF/AO) were used to degrade tetracycline on carbon felt (cathode) and a sub-stoichiometric titanium oxide (Ti<sub>4</sub>O<sub>7</sub>) layer deposited on Ti (anode). As compared to EF and AO, the coupled EF/AO system resulted in the highest pollutant removal efficiencies: total organic carbon removal was 69 ± 1% and 68 ± 1%, at 20 ppm and 50 ppm of initial concentration of tetracycline, respectively. The effect of electrolysis current on removal efficiency, mineralization current efficiency, energy consumption, and solution toxicity of tetracycline mineralization were investigated for 20 ppm and 50 ppm tetracycline. The EF/AO process using a Ti<sub>4</sub>O<sub>7</sub> anode and CF cathode provides low energy and high removal efficiency of tetracycline caused by the production of hydroxyl radicals both at the surface of the non-active Ti<sub>4</sub>O<sub>7</sub> electrode and in solution by the electro-Fenton process at the cathodic carbon felt. Complete removal of tetracycline was observed from HPLC data after 30 min at optimized conditions of 120 mA and 210 mA for 20 ppm and 50 ppm tetracycline concentrations. Degradation products were elucidated, and the toxicity of the products were measured with luminescence using Microtox<sup>®</sup> bacteria toxicity test.

**Keywords:** tetracycline; anodic oxidation; electro-Fenton process; Ti<sub>4</sub>O<sub>7</sub>-ceramic anode; carbon felt; TOC removal efficiency

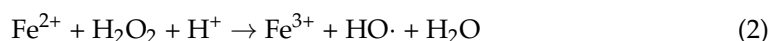
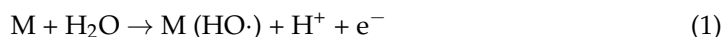
## 1. Introduction

Pharmaceutical compounds have become of special interest in wastewater treatment because of their toxic effects on humans, aquatic lives, and the environment in general even at low concentrations [1–4]. Antibiotics are a class of pharmaceuticals that are extensively used to treat and prevent disease in humans and animals [5]. The concentrations of these antibiotics have been found to range between 116 and 750 ng/L in wastewater influents and 52 to 85 ng/L in effluents, worldwide [6]. The concentration of tetracycline (for example) has been found to be below 10 µg/L in surface water [2]. Tetracycline is an antibiotic used widely for human, animal, and agricultural purposes [3]. Due to the wide usage and

poor absorption of tetracycline, it is excreted through feces and urine and has been found in surface water, ground water, and wastewater in many places around the world [2,7]. Occurrence of antibiotics in the environment is a probable cause of increasing presence of antibiotic resistant genes and bacteria, therefore efficient removal of tetracycline from wastewater is very important [8].

Tetracycline cannot be efficiently removed by biological treatments and techniques such as membrane filtration and adsorption do not break down the tetracycline but only transfers it from one phase to another [5]. Techniques such as advanced oxidation, namely photocatalysis, ozonation, ultrasound, sonoelectrochemistry, and various combinations of advanced technologies such as ultrasound with photocatalysis have been reported as alternative water treatment approaches to the elimination of tetracycline and other recalcitrant organic compounds in wastewater [1,7–10].

Electro-Fenton (EF) and anodic oxidation (AO) are promising water treatment processes under the class of electrochemical advanced oxidation processes (EAOPs) [11–15]. AO can be carried out, via water oxidation, on active or non-active anode of high overvoltage for oxygen evolution reaction, (Equation (1)) [14]. Examples of active anodes include carbon and graphite, iridium-based oxide, platinum-based oxide, etc., while non-active anodes include lead dioxide (PbO<sub>2</sub>) and boron-doped diamond (BDD) [14,15]. Ceramic Ti<sub>4</sub>O<sub>7</sub>, a sub-stoichiometric titanium dioxide of Magnéli phase, has also been identified as an efficient non-active anode for the degradation of recalcitrant substances. Pharmaceuticals like paracetamol were removed up to a maximum of 90% in 8 h, at an initial concentration of 10 ppm [16–19] whereas the removal rate of tetracycline after 120 min of treatment at the current densities of 0.5, 1.0, 2.0, and 3.0 mA cm<sup>−2</sup> was 75.2%, 89.3%, 95.2%, and 97.6%, respectively [17]. For fluoride chemical compounds like perfluoroalkyl substances (PFAS), after 180 min of electrolysis, 93.1 ± 3.4% perfluorooctanesulfonic acid (PFOS) was degraded and 90.3 ± 1.8% TOC was removed [20,21]. A titanium oxide (Ti<sub>4</sub>O<sub>7</sub>) anode generates large amounts of physisorbed hydroxyl radicals (Ti<sub>4</sub>O<sub>7</sub> (HO·)) for the degradation and mineralization of organic contaminants. It also has the potential to become a low-cost anode compared to the well-known boron-doped diamond anode [13,18]. While in AO, hydroxyl radicals are generated at the surface, in the EF process, HO· (hydroxyl radicals) are generated in the bulk through the Fenton's reaction (Equation (2)) where H<sub>2</sub>O<sub>2</sub> and iron (II) are continuously electrogenerated at the cathode by the reduction of dissolved oxygen (Equation (3)) and reduction of iron (III) (Equation (4)), respectively. External oxygen is supplied continuously, and an iron source must be initially added at catalytic amount to the treated solution (homogeneous EF) [12,13].



Homogeneous EF requires an external iron source and acidic pH (2.5–3) that prevents iron (III) precipitation [12]. Carbon felt has been used as a cathode material due to its good electronic conduction and high surface area. It is also very porous which then provides abundant redox reaction sites, combined with a suitable mechanical stability and a relatively low cost [22].

After the degradation process, toxicity tests can be used as an indicator of the acute toxicity of the effluents during the electrochemical treatment. The activity of the living cell could be reduced by the presence of toxic elements. Bioluminescence, which can be used to know the state of bacteria, has been reported for the determination of toxicity of samples [16].

In this study, an EF system with a carbon felt cathode was combined with an AO system with a ceramic Ti<sub>4</sub>O<sub>7</sub> anode to form a combined EF/AO system as depicted in

the scheme in Figure 1. Hydroxyl radicals are produced at both anode (Equation (1)) and cathode (Equations (2)–(4)). The oxygen was supplied to the cathode by the bubbling of air (Figure 1).

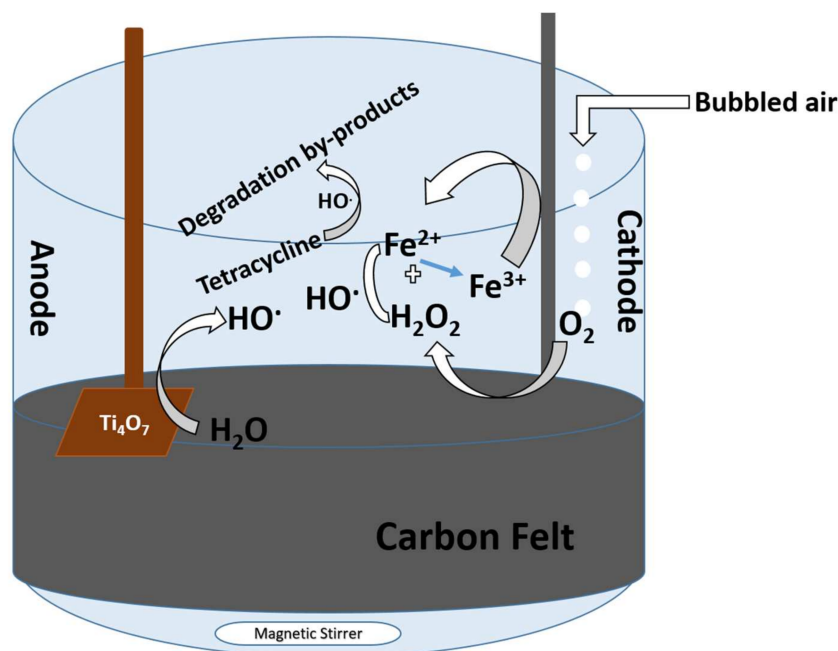


**Figure 1.** Schematic representation of the combined electro-Fenton (EF) and anodic oxidation (AO) system for the degradation of tetracycline.

Using the combined EF/AO system, this study investigates the extent of mineralization, the toxicity of oxidation by-products, and degradation pathways resulting from the degradation of tetracycline. The work further proves the effectiveness of the coupling of the sub-stoichiometric Ti<sub>4</sub>O<sub>7</sub> ceramic anode with carbon felt cathode for water treatment.

## 2. Materials and Methods

### 2.1. Chemicals

Tetracycline (TC), ferrous sulfate (heptahydrate), anhydrous sodium sulfate, organic solvents (HPLC grade), and all other chemicals were purchased from Sigma Aldrich (France) and used as received. All the solutions were prepared with high-purity water obtained from a Millipore MilliQ system with resistivity >18 MΩ·cm at room temperature.

### 2.2. Electrochemical Cell

The experiments were performed in a two-electrode cell system in an undivided cylindrical reactor of 500 mL capacity [19]. The anode is a Ti<sub>4</sub>O<sub>7</sub> thick film deposited on the 2 faces of a Ti substrate (7.5 cm × 4 cm × 0.2 cm) by Saint-Gobain Coating Solution (France). The cathode is a carbon felt (Alfa Aesar, 25 cm × 5 cm × 0.63 cm). Tests were carried out using 230 mL of 0.045 mM (20 ppm TC) and 0.1125 mM (50 ppm TC) (corresponding to 11.88 mg/L and 29.70 mg/L TOC, respectively) in 50 mM Na<sub>2</sub>SO<sub>4</sub> as supporting electrolyte, at room temperature. The anode was centered in the electrochemical cell and surrounded by the cathode, covering the inner wall of the cell. The bubbling of O<sub>2</sub> started 10 min prior the experiments and was maintained throughout the experiments to keep it at a constant concentration. Continuous generation of H<sub>2</sub>O<sub>2</sub> in situ was achieved by 2e<sup>−</sup> reduction of dissolved oxygen at the carbon felt cathode.

### 2.3. Instrument Procedure

Hameg HM8040 was used to supply power to the cell at constant current. Mineralization of the TC in solutions was analyzed from total organic carbon (TOC) measurements

(Shimadzu VCSH TOC analyzer). Reproducible TOC values, within  $\pm 2\%$  accuracy were found using the non-purgeable organic carbon method. The TOC values were used to calculate the mineralization current efficiency according to Equation (5):

$$MCE(\%) = \frac{(\Delta TOC)_{\text{exp}} n F V s}{4.32 \times 10^7 m I t} \times 100 \quad (5)$$

where  $(\Delta TOC)_{\text{exp}}$  ( $\text{mgC.L}^{-1}$ ) is the TOC decay at time  $t$  (h),  $F$  is the Faraday constant ( $96,487 \text{ C mol}^{-1}$ ), vs. is the solution volume (L),  $4.32 \times 10^7$  is a conversion factor ( $=3600 \text{ s h}^{-1} \times 12,000 \text{ mg of C mol}^{-1}$ ),  $m$  is the number of carbon atoms of TC (22 carbon atoms),  $I$  is the applied current (A), and  $n$  is the number of electron consumed per molecule of TC; taken to be 90 assuming complete mineralization of TC into  $\text{CO}_2$ ,  $\text{NH}_4^+$  and  $\text{H}_2\text{O}$  according to Equation (6).



TOC results were also used to determine the energy consumption (EC) expressed as kWh. ( $\text{g TOC}^{-1}$ ) was removed and calculated from Equation (7).

$$EC(\text{kWh} \cdot (\text{g TOC})^{-1}) = \frac{E_{\text{cell}} I t}{V \Delta(TOC)_{\text{exp}}} \quad (7)$$

where  $E_{\text{cell}}$  is the average cell voltage (V),  $I$  the applied current (A),  $t$  the duration of electrolysis (h), vs. the volume of solution treated (mL), and  $\Delta(TOC)_{\text{exp}}$  the experimental decays of TOC ( $\text{mgC.L}^{-1}$ ).

Furthermore, the amount of iron (Fe) in the solution was measured using atomic absorption spectroscopy (AAS) GBC 909 AA (Gbc Scientific; Melbourne, Australia) at a 386.0 nm wavelength and a lamp current of 7.0 mA.

#### 2.4. Toxicity Tests

The toxicity of TC and the intermediate by-products formed during degradation was determined by a Microtox<sup>®</sup> bacteria toxicity test on a Microtox<sup>®</sup> Model 500 Analyzer (Modern Water Inc., London, UK), which measures the luminescence of marine bacteria [21]. The bacteria strain used was *Vibrio fischeri* NRRL B-11177. This bacterium emitted luminescence during growth relating to cellular respiration which is linked to cell activity. The acute toxicity tests results are interpreted by the MicrotoxOmni<sup>®</sup> software, whereas a screening test of 81.9% was used to characterize the inter-sample toxicity variability and identify the relative toxicity of each sample solution in this study. A 22% NaCl solution was used to allow *Vibrio fischeri* normal activity and thus luminescence emission. The pH of samples was adjusted to between 6.5 and 7.5 before the bacteria luminescence analysis using sodium hydroxide (0.1 M NaOH) or sulfuric acid (0.1 M  $\text{H}_2\text{SO}_4$ ).

The inhibition rate at time  $t$ :  $I(t)$  was calculated using Equation (8):

$$i(t)\% = \left(1 - \frac{LU(t)}{LU(0)}\right) \times 100 \quad (8)$$

$LU(0)$  is the initial intensity of luminescence emitted by the bacteria before the addition of the sample.  $LU(t)$  is the intensity of luminescence emitted by bacteria after  $t = 15$  or 30 min of contact with the sample. Since the luminescence of the bacteria decreases over time (in the absence of toxicity), there is need to compensate for the errors due to the variability of the luminescence  $R(t)$  of the bacteria in a control solution (MilliQ water and NaCl) which gives the  $LU(0)$  values, Equation (9).

$$R(t) = \frac{LU_0(t)}{LU_0(0)} \quad (9)$$



The intensity of luminescence emitted by bacteria after a  $t = 15$  or  $30$  min of contact with the control solution (MilliQ water and NaCl) is  $LU_0(t)$ ; while the initial intensity of bacteria luminescence before the addition of the control solution is  $LU_0(0)$ . Equation (10) then depicts the corrected inhibition rate attributed to the toxicity of the sample:

$$Ic(t)\% = \left(1 - \frac{LU(t)}{R(t) \times LU(0)}\right) \times 100 \quad (10)$$

### 2.5. Tetracycline and By-Product Analysis

Tetracycline and its degradation products were analyzed by high-performance liquid chromatography coupled to mass spectrometry (HPLC-MS) with instruments and similar setting as reported in our previous work [10] as follows: HPLC was performed with a Waters 2695 pump, auto sampler with a  $20 \mu\text{L}$  loop, a Waters 2695 separation module (HPLC), a Waters Micromass (Wythenshawe, Manchester, UK) and a Quattro Micro mass spectrometer equipped with electrospray ionization (ESI). For HPLC, Waters-XSelect HSST3  $100 \text{ mm} \times 2.1 \text{ mm}$ ,  $2.5 \mu\text{m}$  particles size with column temperature set at  $25^\circ\text{C}$  was used. Buffer A (HPLC grade water +  $0.1\%$  formic acid) and Buffer B (HPLC grade acetonitrile +  $0.05\%$  formic acid) were used as mobile phase with a constant flow rate of  $0.25 \text{ mL/min}$  to the mass spectrometer. The following isocratic elution profile was applied:  $90\% \text{ A}-10\% \text{ B}$ -Run =  $2 \text{ min}$ . A triple quadrupole MS was operated in selected-ion-monitoring (SIR) mode with compounds being ionized in the negative electrospray ionization mode. For optimum sensitivity, the MS was adjusted to facilitate the ionization process. The detection conditions were: capillary potential  $3.5 \text{ kV}$ , cone potential  $30 \text{ V}$ , source temperature  $120^\circ\text{C}$ , desolvation temperature  $450^\circ\text{C}$ , cone gas flow  $50 \text{ L/h}$ , and desolvation gas flow  $450 \text{ L/h}$ . Nitrogen was used as the nebulizer gas. The limit of detection (LOD) and limit of quantification (LOQ) for  $20 \text{ ppm}$  was  $0.15$  and  $0.45 \text{ ppm}$ , respectively and  $50 \text{ ppm}$  was  $0.18$  and  $0.51 \text{ ppm}$ , respectively.

Oxalic and Oxamic acid were identified by chromatography using a Dionex Thermofisher ICS1000 system with Dionex Thermofisher VWD-3100 UV-Visible detector and a Benson Polymeric BP-OA-2000-0 column at room temperature. The eluent was  $\text{H}_2\text{SO}_4$   $0.05 \text{ N}$  at  $0.4 \text{ mL/min}$ , and the analysis was performed at  $210 \text{ nm}$ .

## 3. Results

### 3.1. Effect of the Combination of Anodic Oxidation and Electro-Fenton Processes on the Mineralization of Tetracycline

EF, AO, and EF/AO experiments were carried out for the mineralization of TC at a constant applied current of  $120 \text{ mA}$  for  $20 \text{ ppm}$  TC and of  $210 \text{ mA}$  for  $50 \text{ ppm}$  TC (Figure 2a,b). For the EF experiment, CF and Pt mesh were used as the cathode and anode respectively in the presence of a  $0.2 \text{ mM}$   $\text{Fe}^{2+}$  catalyst. Whereas in AO,  $\text{Ti}_4\text{O}_7$  and Pt served as anode and cathode respectively without the addition of iron catalyst. Finally, EF/AO was carried out using a  $\text{Ti}_4\text{O}_7$  anode and CF cathode with the addition of  $0.2 \text{ mM}$   $\text{Fe}^{2+}$  catalyst. These experiments were conducted for  $4 \text{ h}$  using  $0.05 \text{ mM}$   $\text{Na}_2\text{SO}_4$  as supporting electrolyte at  $\text{pH } 3$ . After  $240 \text{ min}$  of electrolysis, TOC removal efficiency, for the solution containing  $20 \text{ ppm}$  of TC, was  $41 \pm 1\%$ ,  $62 \pm 1\%$  and  $65 \pm 1\%$  using EF, AO, and EF/AO, respectively. A similar trend was observed with  $50 \text{ ppm}$  TC where  $51 \pm 1\%$ ,  $61 \pm 2\%$  and  $68 \pm 1\%$  TOC removal was recorded using EF, AO, and EF/AO respectively (Table 1).

**Table 1.** Removal % of tetracycline (TC) at  $20 \text{ ppm}$  and  $50 \text{ ppm}$  by the different processes conducted at  $120 \text{ mA}$  for TC  $20 \text{ ppm}$  and  $210 \text{ mA}$  for TC  $50 \text{ ppm}$  during  $4 \text{ h}$ .

	20 ppm			50 ppm		
	EF	AO	EF/AO	EF	AO	EF/AO
% TOC Removal	$41 \pm 1$	$62 \pm 1$	$65 \pm 1$	$51 \pm 1$	$61 \pm 1$	$68 \pm 1$

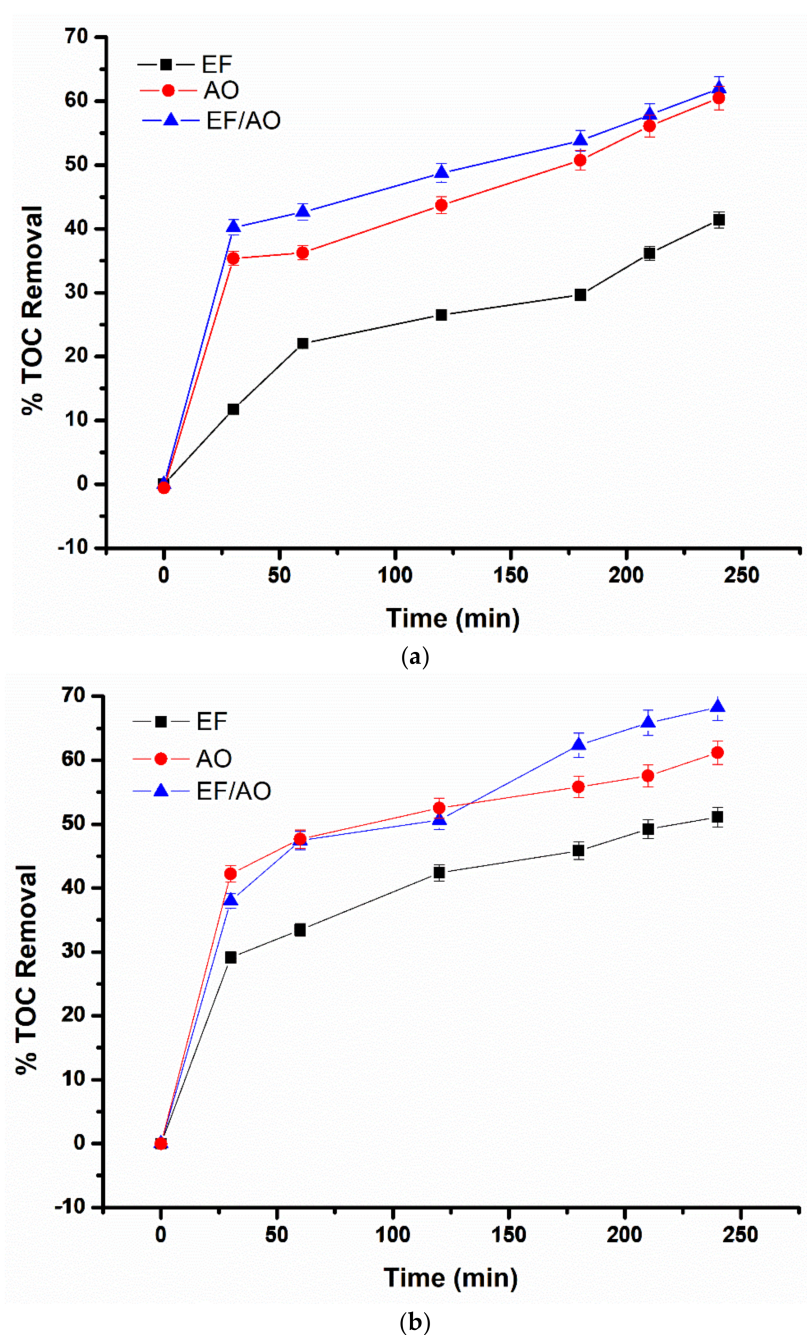


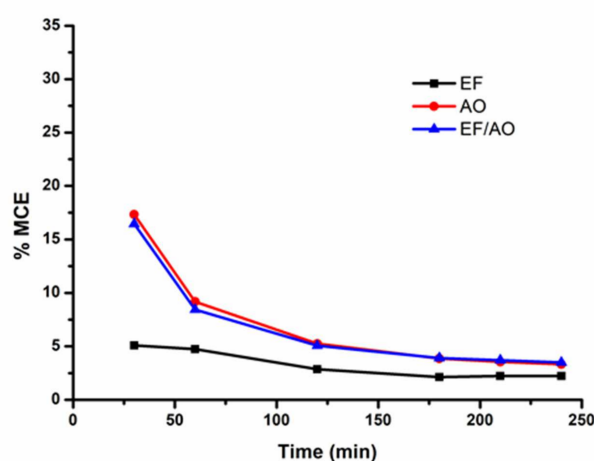
**Figure 2.** Tetracycline mineralization vs. electrolysis time for the degradation of 230 mL of TC at (a) 20 ppm (120 mA) and (b) 50 ppm (210 mA) by EF, AO, and EF/AO.

Regardless of the initial concentration of TC, we noted a sharp increase in the TOC removal in the first hour of electrolysis when operating with EF, AO, and EF/AO. However, the percentage of TOC removal was higher for AO and EF/AO than that of EF throughout the duration of the experiment (Figure 2a,b). There was no marked difference between the percentage of TOC removal for AO and EF/AO in the 20 ppm tetracycline. However, a better performance of the EF/AO is observed at a higher tetracycline concentration of 50 ppm. The 50 ppm concentration will need a higher number of hydroxyl radicals for degradation. Hence, the combined EF/AO generated more radicals for 50 ppm than the AO alone and this explains why the combined method performed better at higher tetracycline concentrations.

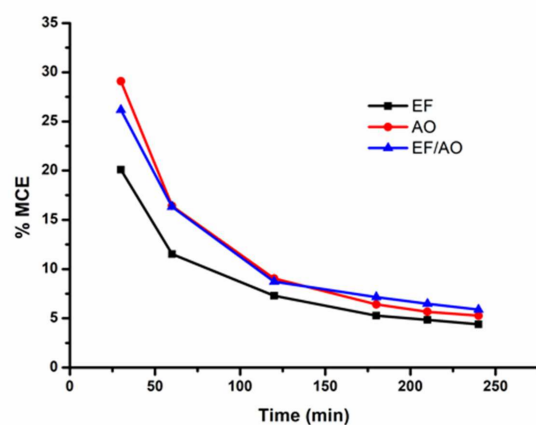
Higher removal efficiency obtained in EF/AO process can rightly be attributed to the combined effect of AO taking place at the  $\text{Ti}_4\text{O}_7$  (anode) surface due to physisorbed hydroxyl radicals and the simultaneous Fenton process happening at the carbon felt cathode. Lin et al. [19] recently showed that TC removal on a Magnéli phase  $\text{Ti}_4\text{O}_7$  porous anode was mainly due to reactions mediated by hydroxyl radical production. For a combined method such as AO/EF, a high mineralization rate of TC on BDD by coupling AO/EF on BDD or Pt at the anode and cathodic heterogeneous electro-Fenton process, have been reported [23]. It has been shown that the replacement of Pt anode with a cheaper  $\text{Ti}_4\text{O}_7$  anode facilitated the production of physisorbed hydroxyl radicals due to its high overvoltage for oxygen evolution reaction (OER potential  $> 0.7$  V) compared to the Pt anode (OER potential  $< 0.4$  V) [17]. To go further considering the equipment cost of the system, it is evident that the replacement of BDD anodes by cost-effective  $\text{Ti}_4\text{O}_7$  electrodes will be of great interest.

### 3.2. Mineralization Current Efficiency and Energy Consumption of the Coupled Process

Mineralization current efficiency (MCE) was calculated during the removal of 20 and 50 ppm TC at 120 mA and 210 mA, respectively for EF, AO, and EF/AO (Figure 3a,b). A similar trend to TOC removal in Figure 2 is observed where the MCE is highest for the combined EF/AO especially at a 50 ppm concentration (Figure 3b). This is due to the production of hydroxyl radicals at the surface of the anode which can oxidize TC more efficiently.



(a)



(b)

**Figure 3.** Tetracycline MCE vs. time for the degradation of 230 mL of TC at (a) 20 ppm (120 mA) and (b) 50 ppm (210 mA) by EF, AO, and EF/AO.

Regardless of the process (EF, AO, or EF/AO) and the anode materials used, the MCE progressively decayed over time at 20 ppm and 50 ppm TC concentrations (Figure 3). This decay is due to (i) the reduction in the concentration of organic matter in the solution that can lead to reduction in mass transport, (ii) the formation of more recalcitrant degradation by-products which are more difficult to for the hydroxyl radical to oxidize, and (iii) the reduction in the concentration of HO/M(HO·) in the solution as a result of the formation of scavengers which can compete with the oxidation of organic matter [24–26].

The combination of EF/AO was used for all the following experiments because of the interest of the coupling previously demonstrated. Additionally, investigations of the effect of different applied currents on the energy consumption (EC), at 20 and 50 ppm TC, were carried out (Table 2). The results presented in Table 2 show that, at a given time, the higher current density, the more energy consumption required. For the highest current density at 20 ppm TC, this is mainly related to the cell voltage increase because  $\Delta(\text{TOC})_{\text{exp}}$  is almost constant (Figure 4a).

Figure 4a,b present the TOC removal for the coupled process as a function of time. There was a significance increase in TOC removal when current was increased from 80 mA to 120 mA than when increased from 120 mA to 300 mA for 20 ppm especially (Figure 4a). Figure 4b also shows a similar trend of higher TOC increase from 120 mA to 210 than from 210 mA to 300 mA. This is due to reduction in the oxidation ability of the processes due to progressive enhancement of parasitic reactions for high current values that consume the generated hydroxyl radicals without contributing efficiently to the mineralization of organics and then decrease MCE [16]. This could also be due to the loss of hydroxyl radicals because of dimerization to form  $\text{H}_2\text{O}_2$  or production of hydroxyl ions upon reaction with ferrous ions. A major reason for the TOC removal trend observed with the use of 80 mA is partly due to the insufficient current to facilitate the generation of substantial oxidants for the degradation. We measured the amount of iron present in the solution at time intervals and a decrease in the concentration of iron was observed after 30 min. The reduction in iron could have been due to the iron-scavenging effect of oxalic acid by-product. Thus, in addition to the low current, the TOC removal at 80 mA is also due to the low concentration of iron in the solution. The low concentration of iron could not generate the needed amount of hydroxyl radicals. However, at higher currents more oxidants were being produced before the inhibition of iron could happen.

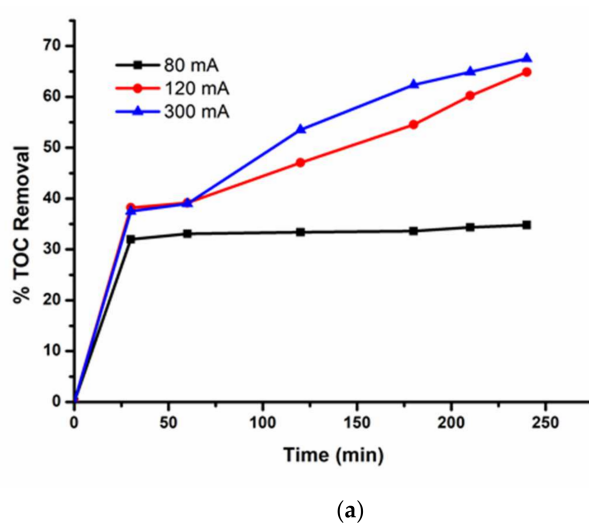
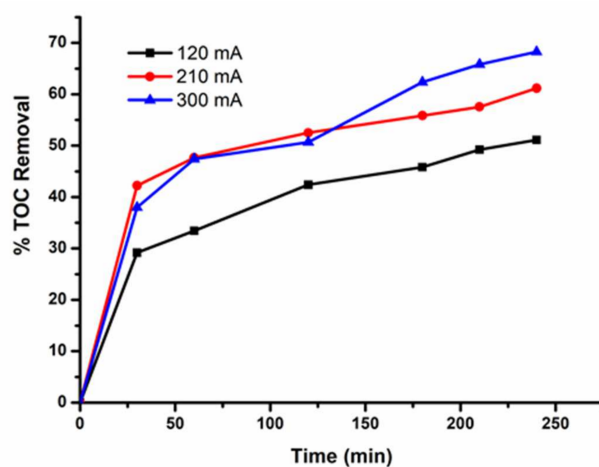
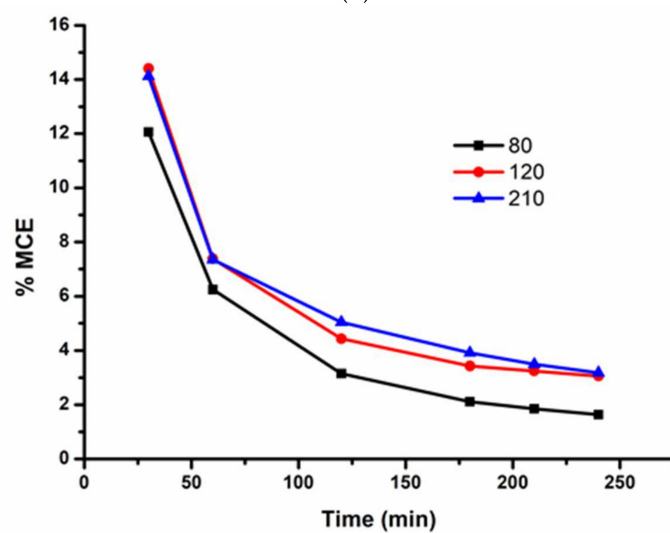


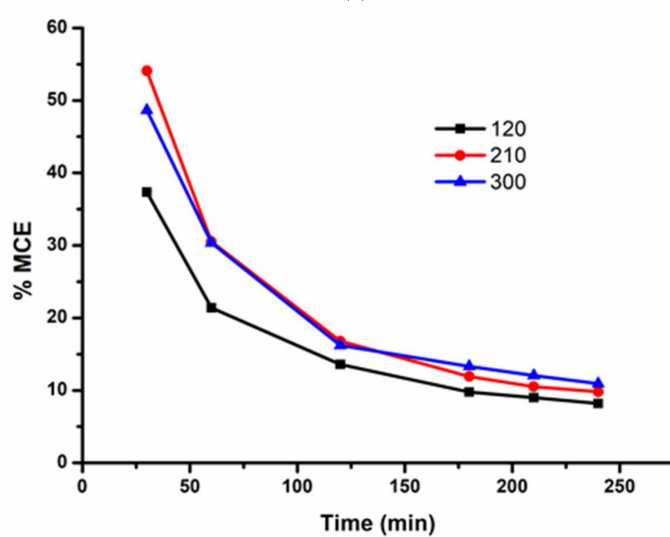
Figure 4. Cont.



(b)



(c)



(d)

**Figure 4.** Tetracycline mineralization efficiency of EF/AO at different current on TC solutions in 0.05 M Na<sub>2</sub>SO<sub>4</sub> at pH 3 using Ti<sub>4</sub>O<sub>7</sub> anode (a) %TOC removal for 20 ppm TC, (b) %TOC removal for 50 ppm TC, (c) %MCE for 20 ppm TC and (d) %MCE for 50 ppm TC.



**Table 2.** Energy consumption (EC) for the removal of 20 and 50 ppm tetracycline after 4 h of treatment by the coupled EF/AO process.

	20 ppm			50 ppm		
Current (mA)	80	120	300	120	210	300
TOC Removal (%)	35	65	67	51	61	68
EC (kWh (g TOC <sup>−1</sup> ))	0.14	0.11	0.21	0.05	0.08	0.12

In the same way, an increase in applied current from 80 to 120 mA for 20 ppm (Figure 3b) or from 120 to 210 mA for 50 ppm (Figure 4d) led to an increase in MCE, indicating that the hydroxyl radicals were used efficiently in the oxidation of organic molecules, thus minimizing side reactions [27]. It is also worth noting that for 20 ppm TC, the TOC removal reaches a plateau if applying a current of 80 mA definitely because of the low production of radicals for mineralization of 20 ppm TC at this current value as explained earlier. Based on these results, an applied current of 120 and 210 mA for an efficient removal of tetracycline at 20 ppm and 50 ppm respectively seems to be the best compromise to get a high removal rate, low EC, and high MCE. The measurements done for iron for 120 mA and 210 mA, 20 and 50 ppm, respectively, have proved that more hydroxyl radicals were formed because the iron concentration was high. The current applied was able to convert the ferric ions into active ferrous ions.

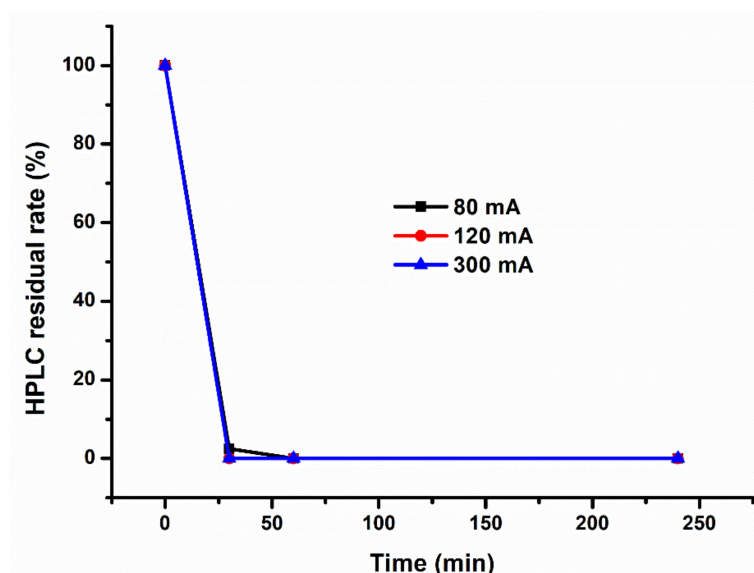
### 3.3. Tetracycline Degradation and By-Products Identification Using EF/AO Process

The monitoring of tetracycline concentration by HPLC-MS further proved that the current value applied to the electrochemical cell plays a major role not only for TOC removal, but also for fast organic pollutant degradation. For 20 ppm TC (Figure 5a), an applied current of 80 mA resulted in 97.5% tetracycline removal (i.e., 2.5% of residual TC) after 30 min. However, there was no TC detected after 1 h with applied currents of 80, 120, and 300 mA. A complete disappearance of the pollutant was then achieved in a very short time Yahiaoui et al. [28] and Wu et al. [29] also reported a complete disappearance of TC, however, with different approaches. For 50 ppm (Figure 5b), a complete degradation of TC was observed for 120 mA at 4 h, for 210 mA at 3.5 h, and for 300 mA at 30 min.

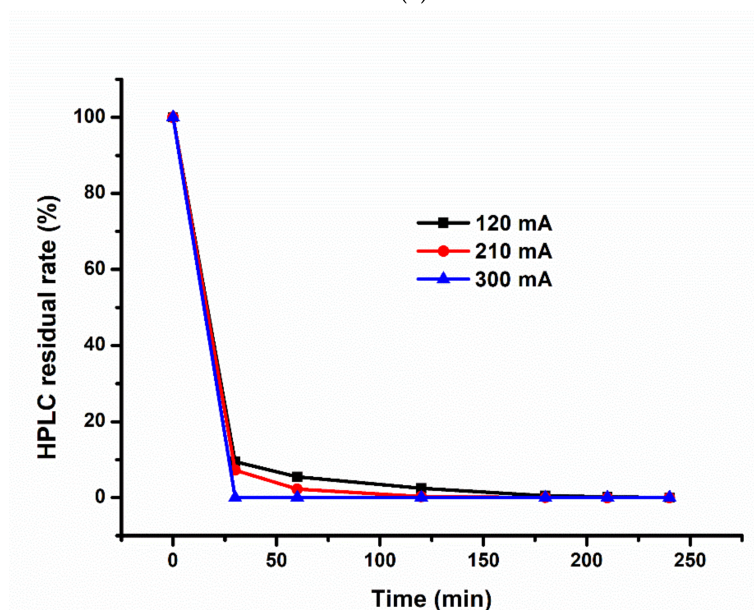
Three degradation by-products (P1, P2, and P3) of TC were identified during the process and summarized Table 3 for the treatment of 20 ppm of TC at 120 mA and 50 ppm of TC at 210 mA (previously identified as the optimized currents). At 30 min, P1 represents the main by-product,  $81 \pm 1\%$ , whatever the initial concentration of TC. P1 has been identified by Dalmazio et al. [30] during the monitoring of the degradation of tetracycline by ozone in aqueous medium. After 30 min, P2 was identified in the solution at 20 ppm TC initial concentration at  $52 \pm 1\%$  (i.e.,  $P1\ 48 \pm 1\%$ ), whereas P3 was identified only in the solution at 50 ppm at  $50 \pm 1\%$  (i.e.,  $P1\ 50 \pm 1\%$ ). It should be noted that none of them were detected at 60 min of electrolysis, which proves their fast degradation as intermediate products.

The mass spectrometry in the positive ion mode, ESI(+)-MS (Table 3), shows that TC, detected in its protonated form ( $[1 + H]^+$ ) of  $m/z\ 445$ , reacted to yield two products. These products are P1 and P2 for 20 ppm and P1 and P3 for 50 ppm (Figure 6). The P1 product was identified for both 20 and 50 ppm. The isomer of TC which is P1 happened at C22, the exchange of amine group with carbonyl and formed a hydroxyl. Compound P2 from P1, produced by demethylation at C3, removal of the methanol group at C3, addition of alkoxy group ( $-O-CH_3$ ) at C5, removal of carbonyl O at C8 (ketone removal), substitution of amine group with carbonyl group at C22, addition of methyl group in exchange of OH at C22, hydrolysis (reduction) of ketone at C10 to OH, oxidation at C12 from alcohol to ketone and reduction at C14 from ketone to OH. From isomer to P3, the following formations happened, substitution of secondary amine with an alkyl group at C7 (substitution of N with C), addition of carbonyl (ketone) oxygen; oxidation at C8, C10, C12, C14, same as P2 and then alkylation at C1 (addition of ethyl group). Other studies using HPLC-ESI-Q-

TOF-MS/MS to determine the photodegradation products of TC in UV direct photolysis indicated that TC still contained the characteristic structure of tetra-phenyl though some of their substituent groups changed, resulting in a lower steric resistance [31].



(a)



(b)

**Figure 5.** Applied current effect on tetracycline residual rate (in %) determined by HPLC-MS for (a) 20 ppm TC at 80, 120, and 300 mA and (b) 50 ppm TC at 120, 210, and 300 mA using the EF/AO ( $\text{Ti}_4\text{O}_7$  anode) process.

**Table 3.** Mass spectrometry data of TC degradation products.

Product	Short Written	Elemental Composition	Measured Mass (M)
TC	(M)+	$\text{C}_{22}\text{H}_{24}\text{N}_2\text{O}_8$	444.4
P1	(M + H)+	$\text{C}_{22}\text{H}_{25}\text{N}_2\text{O}_8$	445.4
P2 (20 ppm)	(M-N + CH)	$\text{C}_{23}\text{H}_{26}\text{NO}_8$	443.4
P3 (50 ppm)	(M-N + CH)	$\text{C}_{23}\text{H}_{26}\text{NO}_8$	443.4

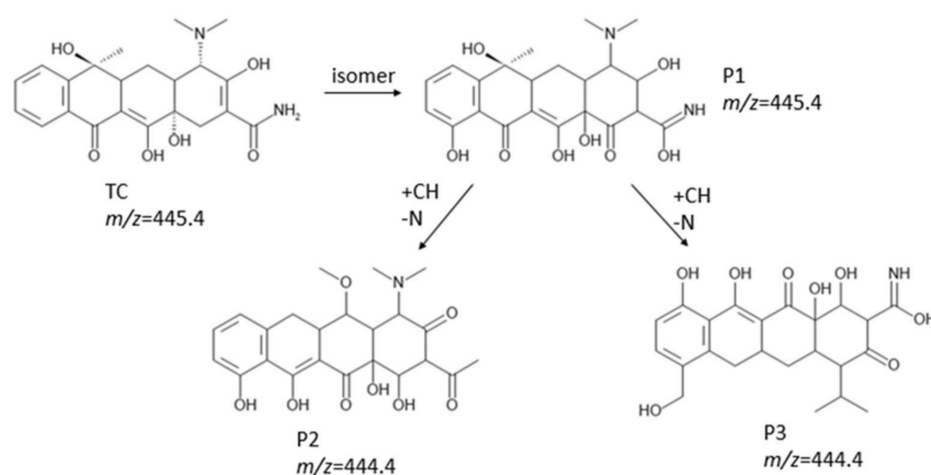


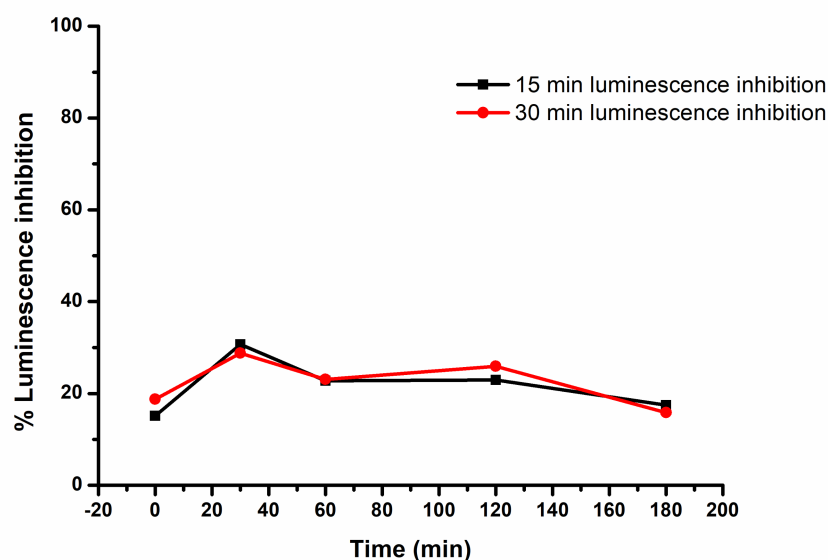
**Figure 6.** Possible reaction pathways based on molecular weight of TC by-products identified by LC-MS. Pathways TC/P1/P2 and TC/P1/P3 for the solution at 20 ppm and 50 ppm TC initial concentration respectively.

Furthermore, short-chain carboxylic acids were identified from the degradation of the above by-products (P1, P2, and P3) from 1 h to 4 h treatment time. The carboxylic acids by-products shown in the chromatograms were oxalic and oxamic acids. After 4 h, oxalic acid was detected at  $1.20 \text{ mg L}^{-1}$  and  $1.55 \text{ mg L}^{-1}$  which represent 9.9% and 5.0% of the initial carbon content for 20 ppm TC and 50 ppm TC initial solutions, respectively. In the same way, after 4 h, oxamic acid was detected at  $0.88 \text{ mg L}^{-1}$  and  $1.48 \text{ mg L}^{-1}$  which represent 7.2% and 4.8% of the initial carbon content for 20 ppm TC and 50 ppm TC of the initial solutions, respectively. Obviously, C content of the identified carboxylic acids (i.e., oxalic and oxamic) represents only 17.1% and 9.8% of the initial C content of the solution for 20 ppm TC and 50 ppm TC, respectively. Whereas Yuan et al. (2011) found that TC initial by-products were more toxic than the short carboxylic acids which can be degraded easily biologically. These non-toxic by-products include hydroxymalonic acid, 1, 4-benzenedicarboxylic acid, propanedioic acid, 4-oxo-pentanoic acid, glycerin, some aliphatic acids, etc. which were determined by GC-MS analysis. All these identified compounds were unequivocally identified using the NIST98 library database with fit values higher than 90% [31].

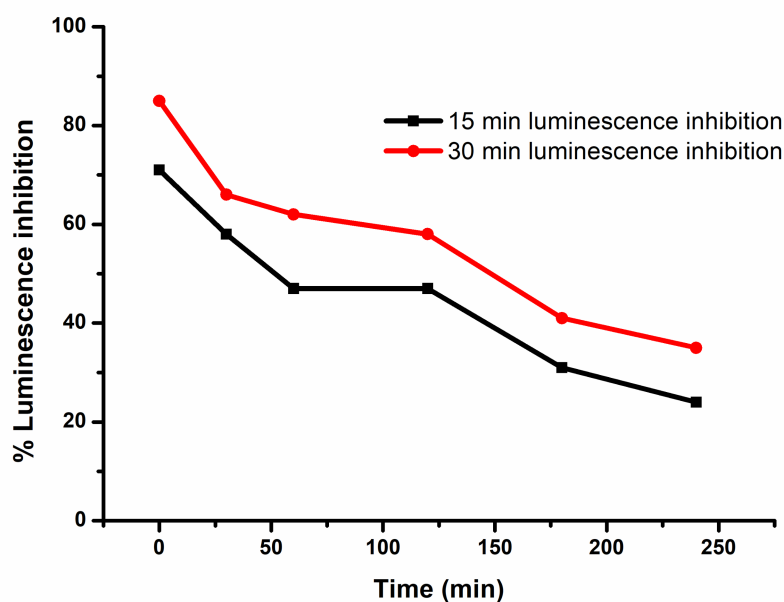
### 3.4. Toxicity Assessment during Tetracycline Degradation Using EF/AO Process

The toxicity evolution of 230 mL of 20 ppm and 50 ppm TC treated at 120 mA and 210 mA respectively were measured by monitoring the luminescence inhibition of the marine bacteria *Vibrio fischeri* after 15 min and 30 min of exposure. The average values of luminescence inhibition after 15 and 30 min of exposure are given as a function of electrolysis time (Figure 7). A solution with an initial TC concentration of 20 ppm (Figure 7a) showed an initial increase in toxicity at  $t = 30 \text{ min}$  after 15 min of exposure time, then a decrease which indicates that the initial by-products mix is more toxic than the following by-products for the solution at initial TC concentration of 20 ppm. The % inhibition luminescence  $LD_{50}$  values for 20 ppm TC at 15 min and 30 min, were 21.60 and 22.15, respectively. However, for the TC solution at 50 ppm, at  $t = 30 \text{ min}$  the by-products showed less toxicity as compared to the initial TC concentration (Figure 7b). In this case the toxicity of the initial product was high compared to the final by-products, which indicates a gradual decrease in toxicity with electrolysis. It shows that toxicity decreased from 58% to 19% inhibition and from 70% to 28% for 15 min and 30 min of exposure time, respectively. Where the % inhibition luminescence  $LD_{50}$  for 50 ppm TC, at 15 min and 30 min was 49.02 and 60.58, respectively. The decrease in the solution toxicity proved that the intermediate products formed are less toxic than the initial TC sample. Based on Figure 7a,b we can then conclude (i) the measurements of luminescence inhibition is reliable because of the

good correlation for measurements after 15 min and 30 min of exposure time for each solution (i.e., 20 and 50 ppm), (ii) in as little as 30 min of electrolysis time, the electrochemical advanced oxidation process induces a decrease of the toxicity, (iii) the toxicity of the solution increase with the TC concentration, and (iv) a threshold effect is observed between 20 and 50 ppm of TC because of the huge increase of the initial TC toxicity at 50 ppm compared to 20 ppm (i.e., 70 to 85% luminescence inhibition and 15 to 19% for 50 and 20 ppm respectively as proved by Figure 7a,b).



(a)



(b)

**Figure 7.** Growth of the inhibition of marine bacteria luminescence of 20 ppm (a) and 50 ppm (b). TC taken after different EF/AO treatment. RSD ( $n = 3$ ): 12% for inhibition < 20%; 5% for 20% < inhibition < 70% and 0% for inhibition > 70%.

#### 4. Conclusions

The mineralization of tetracycline by electrochemical advanced oxidation processes (EAOPs) using  $\text{Ti}_4\text{O}_7$  as anode and carbon felt as the cathode was successful. The complete elimination of tetracycline was achieved after 30 min of electrolysis for both 20 and 50 ppm. The results for TOC removal using different EAOPs showed that EF/AO ( $65 \pm 1\%$  and  $68 \pm 1\%$ , TOC removal at 20 ppm and 50 ppm TC, respectively) was more efficient compared to EF (TOC removal  $41 \pm 1\%$  and  $51 \pm 1\%$  at 20 ppm and 50 ppm, respectively) and AO (TOC removal  $62 \pm 1\%$  and  $61 \pm 1\%$  at 20 ppm and 50 ppm, respectively). The optimal applied current was 120 mA and 210 mA, for 20 ppm and 50 ppm, respectively when using the EF/AO process. Applied current plays a major role in degradation of organic pollutants. The higher the applied current the higher TOC removal. The identification and evolution of intermediate products, as well as the toxicity of the solution were also examined along the EF/AO process. After 30 min treatment time, P1 by-product was identified at  $81 \pm 1\%$  for both 20 ppm (120 mA) and 50 ppm (210 mA) TC initial concentration. Then a mix of P1 ( $52 \pm 1\%$ ) and P2 ( $48 \pm 1\%$ ) and P1 ( $50 \pm 1\%$ ) and P3 ( $50 \pm 1\%$ ) were identified for the solution of 20 ppm and 50 ppm TC initial concentration respectively. These by-products produced smaller carboxylic acids (oxamic and oxalic) leading to a decrease in the toxicity of the initial TC solution showing that  $\text{Ti}_4\text{O}_7$  can be used as an efficient and cost-effective anode in EF/AO processes for the mineralization of pharmaceuticals.

**Author Contributions:** Conceptualization, M.C. and O.A.A.; funding acquisition, O.A.A.; investigation, B.N.Z., C.G., E.P. and V.B.; methodology, B.N.Z., B.O.O., E.P., V.B., G.L., M.R., M.C. and O.A.A.; resources, M.C. and O.A.A.; supervision, N.M., M.C. and O.A.A.; writing—original draft, B.N.Z.; writing—review and editing, B.O.O., B.A.K., N.M., C.G., G.L., M.R., M.C. and O.A.A. All authors have read and agreed to the published version of the manuscript.

**Funding:** The authors gratefully acknowledge the following institutions in South Africa for funding: The National Research Foundation (CPRR Grant number: 118546); Water Research Commission (Grant Number: K5/2567); Centre for Nanomaterials Science Research, University of Johannesburg; Faculty of Science, University of Johannesburg; DST/Mintek Nanotechnology Innovation Centre, University of Johannesburg (UJ).

**Institutional Review Board Statement:** Not applicable.

**Informed Consent Statement:** Not applicable.

**Data Availability Statement:** The data presented in this study are available on request from the corresponding author.

**Conflicts of Interest:** The authors declare no conflict of interest.

#### References

1. Daghrir, R.; Drogui, P. Tetracycline antibiotics in the environment: A review. *Environ. Chem. Lett.* **2013**, *11*, 209–227. [\[CrossRef\]](#)
2. Kanama, K.M.; Daso, A.P.; Mpenyana-Monyatsi, L.; Marthie, A.A.; Coetzee, M.A.A. Assessment of pharmaceuticals, personal care products, and hormones in wastewater treatment plants receiving inflows from health facilities in North West Province, South Africa. *J. Toxiloc.* **2018**, *2018*, 3751930. [\[CrossRef\]](#)
3. Rogowska, J.; Cieszyńska-Semenowicz, M.; Ratajczyk, W.; Wolska, L. Micropollutants in treated wastewater. *Ambio* **2020**, *49*, 487–503. [\[CrossRef\]](#)
4. Palominos, R.A.; Mondaca, M.A.; Giraldo, A.; Peñuela, G.; Pérez-Moya, M.; Mansilla, H.D. Photocatalytic oxidation of the antibiotic tetracycline on  $\text{TiO}_2$  and  $\text{ZnO}$  suspensions. *Catal. Today* **2009**, *144*, 100–105. [\[CrossRef\]](#)
5. Zelalem, B.; Meareg, A. Recent reports on electrochemical determination of selected antibiotics in pharmaceutical formulations: A mini review. *Electrochem. Commun.* **2020**, *121*, 106863.
6. Hubeny, J.; Harnisz, M.; Korzeniewska, E.; Buta, M.; Zieliński, W.; Rolbiecki, D.; Giebułtowski, J.; Nałęcz-Jawecki, G.; Płaza, G. Industrialization as a source of heavy metals and antibiotics which can enhance the antibiotic resistance in wastewater, sewage sludge and river water. *PLoS ONE* **2021**, *16*, e0252691. [\[CrossRef\]](#)
7. Patel, M.; Kumar, R.; Kishor, K.; Mlsna, T.; Pittman, C.U., Jr.; Mohan, D. Pharmaceuticals of emerging concern in aquatic systems: Chemistry, occurrence, effects, and removal methods. *Chem. Rev.* **2019**, *119*, 3510–3673. [\[CrossRef\]](#) [\[PubMed\]](#)
8. Gopal, G.; Alex, S.A.; Chandrasekaran, N.; Mukherjee, A. A review on tetracycline removal from aqueous systems by advanced treatment techniques. *RSC Adv.* **2020**, *10*, 27081–27095. [\[CrossRef\]](#)



9. Gangadhar, A.; Ekaterina, V.R.; Rominder, P.S.S. Evaluation of relative importance of ultrasound reactor parameters for the removal of estrogen hormones in water. *Ultrason. Sonochem.* **2012**, *19*, 953–958.
10. Theerthagiri, J.; Lee, S.J.; Karuppasamy, K.; Arulmani, S.; Veeralakshmi, S.; Ashokkumar, M.; Choi, M.Y. Application of advanced materials in sonophotocatalytic processes for the remediation of environmental pollutants. *J. Hazard. Mater.* **2021**, *412*, 125245. [[CrossRef](#)] [[PubMed](#)]
11. Orimolade, B.O.; Zwane, B.N.; Koiki, B.A.; Rivallin, M.; Bechelany, M.; Mabuba, N.; Lesage, G.; Cretin, M. Coupling cathodic electro-fenton with anodic photo-electrochemical oxidation: A feasibility study on the mineralization of paracetamol. *J. Environ. Chem. Eng.* **2020**, *5*, 104394. [[CrossRef](#)]
12. Oturan, M.A.; Aaron, J.J. Advanced oxidation processes in water/wastewater treatment: Principles and applications. A review. *Crit. Rev. Environ. Sci. Technol.* **2014**, *44*, 2577–2641. [[CrossRef](#)]
13. Brillas, E.; Sirés, I.; Oturan, M.A. Electro-fenton process and related electrochemical technologies based on fenton's reaction chemistry. *Chem. Rev.* **2009**, *109*, 6570–6631. [[CrossRef](#)] [[PubMed](#)]
14. Trellu, C.; Oturan, N.; Pechaud, Y.; Hullebusch, E.D.; Esposito, G.; Oturan, M.A. Anodic oxidation of surfactants and organic compounds entrapped in micelles—Selective degradation mechanisms and soil washing solution reuse. *Water Res.* **2017**, *118*, 1–11. [[CrossRef](#)]
15. Panizza, M.; Brillas, E.; Comninellis, C. Application of boron-doped diamond electrodes for wastewater treatment. *J. Environ. Eng. Manag.* **2008**, *18*, 139–153.
16. Ouada, Y.; Trellu, C.; Lesage, G.; Rivallin, M.; Drogui, P.; Cretin, M. Electro-oxidation of secondary effluents from various wastewater plants for the removal of acetaminophen and dissolved organic matter. *Sci. Total Environ.* **2020**, *738*, 140352. [[CrossRef](#)]
17. Ganiyu, S.O.; Oturan, N.; Raffy, S.; Cretin, M.; Causserand, C.; Oturan, M.A. Efficiency of plasma elaborated sub-stoichiometric titanium oxide (Ti<sub>4</sub>O<sub>7</sub>) ceramic electrode for advanced electrochemical degradation of paracetamol: In different electrolyte media. *Sep. Pur. Technol.* **2019**, *208*, 142–152. [[CrossRef](#)]
18. Ganiyu, S.O.; Oturan, N.; Raffy, S.; Esposito, G.; Hullebusch, E.D.; Cretin, M.; Oturan, M.A. Use of sub-stoichiometric titanium oxide as a ceramic electrode in anodic oxidation and electro-fenton degradation of the beta-blocker propranolol: Degradation kinetics and mineralization pathway. *Electrochim. Acta* **2017**, *242*, 344–354. [[CrossRef](#)]
19. Lin, H.; Niu, J.; Liang, S.; Wang, C.; Wang, Y.; Jin, F.; Luo, Q.; Huang, Q. Development of macroporous Magnéli phase Ti<sub>4</sub>O<sub>7</sub> ceramic materials: As an efficient anode for mineralization of poly- and perfluoroalkyl substances. *Chem. Eng. J.* **2018**, *354*, 1058–1067. [[CrossRef](#)]
20. Liang, S.; Lin, H.; Yan, X.; Huang, Q. Electro-oxidation of tetracycline by a Magnéli phase Ti<sub>4</sub>O<sub>7</sub> porous anode: Kinetics, products, and toxicity. *Chem. Eng. J.* **2018**, *332*, 628–636. [[CrossRef](#)]
21. Le, T.X.H.; Haflich, H.; Amisha DShah, A.D.; Chaplin, B.P. Energy-efficient electrochemical oxidation of perfluoroalkyl substances using a Ti<sub>4</sub>O<sub>7</sub> reactive electrochemical membrane anode. *Environ. Sci. Technol. Lett.* **2019**, *6*, 504–510. [[CrossRef](#)]
22. Le, T.X.H.; Bechelany, M.; Cretin, M. Carbon felt based-electrodes for energy and environmental applications: A review. *Carbon* **2017**, *122*, 564–591.
23. Chen, T.S.; Tsai, R.W.; Chen, Y.S.; Huang, K.L. Electrochemical degradation of tetracycline on BDD in aqueous solutions. *Int. J. Electrochem. Sci.* **2014**, *9*, 8422–8434.
24. Le, T.X.H.; Nguyen, T.V.; Yacouba, Z.A.; Zoungrana, L.; Avril, F.; Petit, E.; Mendret, J.; Bonniol, V.; Bechelany, M.; Lacour, S.; et al. Toxicity removal assessments related to degradation pathways of azo dyes: Toward an optimization of electro-fenton treatment. *Chemosphere* **2016**, *161*, 308–318. [[CrossRef](#)]
25. Barhoumi, N.; Olvera-Vargas, H.; Oturan, N.; Huguenot, D.; Gadri, A.; Ammar, S.; Brillas, E.; Oturan, M.A. Kinetics of oxidative degradation/mineralization pathways of the antibiotic tetracycline by the novel heterogeneous electro-Fenton process with solid catalyst chalcopyrite. *Appl. Catal. B Environ.* **2017**, *209*, 637–647. [[CrossRef](#)]
26. Ganiyu, S.O.; Oturan, N.; Trellu, C.; Raffy, S.; Cretin, M.; Causserand, C.; Oturan, M.A. Abatement of analgesic antipyretic 4-aminophenazone using conductive boron-doped diamond and sub-stoichiometric titanium oxide anodes: Kinetics, mineralization and toxicity assessment. *ChemElectroChem* **2019**, *6*, 1808–1817. [[CrossRef](#)]
27. Sirés, I.; Oturan, N.; Oturan, M.A. Electrochemical degradation of  $\beta$ -blockers. Studies on single and multicomponent synthetic aqueous solutions. *Water Res.* **2010**, *44*, 3109–3120. [[CrossRef](#)]
28. Yahiaoui, I.; Aissani-Benissad, F.; Fourcade, F.; Amrane, A. Removal of tetracycline hydrochloride from water based on direct anodic oxidation (Pb/PbO<sub>2</sub> electrode) coupled to activated sludge culture. *Chem. Eng. J.* **2013**, *221*, 418–425. [[CrossRef](#)]
29. Wu, J.; Zhang, H.; Oturan, N.; Wang, Y.; Chen, L.; Oturan, M.A. Application of response surface methodology to the removal of the antibiotic tetracycline by electrochemical process using carbon-felt cathode and DSA (Ti/RuO<sub>2</sub>–IrO<sub>2</sub>) anode. *Chemosphere* **2012**, *87*, 614–620. [[CrossRef](#)] [[PubMed](#)]
30. Dalmázio, I.; Almeida, M.O.; Augusti, R.; Alves, T.M.A. Monitoring the degradation of tetracycline by ozone in aqueous medium via atmospheric pressure ionization mass spectrometry. *J. Am. Soc. Mass Spectrom.* **2007**, *18*, 679–687. [[CrossRef](#)]
31. Yuan, F.; Hu, C.; Hu, X.; Wei, D.; Chen, Y.; Qu, J. Photodegradation and toxicity changes of antibiotics in UV and UV/H<sub>2</sub>O<sub>2</sub> process. *J. Hazard. Mater.* **2011**, *185*, 1256–1263. [[CrossRef](#)] [[PubMed](#)]